

FRACTURE OF FRP IN MARINE APPLICATIONS:
CONSTANT LOAD CRACK PROPAGATION

William Douglas Bartron

Library
Naval Postgraduate School
Monterey, California 93940

FRACTURE OF FRP IN MARINE APPLICATIONS:

CONSTANT LOAD CRACK PROPAGATION

by

WILLIAM DOUGLAS BARTRON

B.S.(O.E.), United States Naval Academy

1973

SUBMITTED IN PARTIAL FULFILLMENT

OF THE REQUIREMENTS FOR THE

DEGREE OF

MASTER OF SCIENCE IN

OCEAN ENGINEERING

at the

Massachusetts Institute of Technology

May, 1974

Thesis

B242346

FRACTURE OF FRP IN MARINE APPLICATIONS:

CONSTANT LOAD CRACK PROPAGATION

by

WILLIAM DOUGLAS BARTRON

Submitted to the Department of Ocean Engineering on 10 May 1974,
in partial fulfillment of the requirements for the degree of Master of
Science in Ocean Engineering.

ABSTRACT

A particular FRP laminate is examined experimentally in air and when submerged in distilled water. The experimentally obtained strength-time curves are presented. These curves indicate that the submerged static life of the material is a constantly decreasing percentage of the dry environment static life as the stress level decreases.

The effect of submerging the material in distilled water is to slow the rate of crack growth. The relationship between the constant load crack propagation rate and stress intensity factor is identified experimentally for both the dry and submerged environments. The mechanism of the growth is confirmed to be that of discrete ligament failures.

A theory is proposed and examined for predicting the crack propagation rate. The initial theory is then modified to approximate the observed data. Further experimental work is recommended to examine the theory more closely.

Thesis Supervisor: Frederick J. McGarry

Title: Professor, Department of Civil Engineering

ACKNOWLEDGEMENTS

I wish to express my sincere appreciation to Professor Frederick J. McGarry, Department of Civil Engineering, Massachusetts Institute of Technology, for his advice, guidance, and encouragement in all areas of this work. I am also very deeply indebted to Doctor John Mandell of the same department whose experience, knowledge, and guidance were invaluable in the successful completion of this work.

The instruction, advice, and assistance of Mr. Arthur Rudolph were immensely helpful in the machining of the specimens, alterations to the water containment system, and construction of the timing device. I am also indebted to graduate students Conrad Fong, Dario Gasparini, and Jorge Alva-Hurtado for lending me their time and equipment for this work. I am especially indebted to graduate student Reiichiro Kashihara for his continued help and advice throughout this study.

I wish to extend a special note of thanks to my wife, Beth, for her support, and tolerance of unusual hours, through the many months of experimentation as well as for her patience and perseverance in typing this work.

TABLE OF CONTENTS

	Page
Title Page	1
Abstract	2
Acknowledgements	3
Table of Contents	4
List of Symbols	5
I. Introduction	6
II. Materials	8
III. Experimental Procedure	10
IV. Analytical Method	13
V. Results	16
VI. Discussion of Results	18
VII. Conclusions	20
VIII. Recommendations	22
References	24
Appendices	25
List of Figures	26
List of Tables	37

LIST OF SYMBOLS

- B = Specimen thickness - inches
- c = Crack length measured from center line of applied load - inches
- d = Ligament size - inches
- $\frac{dc}{dt}$ = Crack propagation rate - inches/minute
- H = Index card specimen half-width - inches
- K_I = Opening mode stress intensity factor - $\text{ksi-in}^{\frac{1}{2}}$
- K_Q = Critical stress intensity factor - $\text{ksi-in}^{\frac{1}{2}}$
- P = Applied load - lb
- s = Slope of linear s-t curve - psi/decade of minutes
- t = Time - minutes
- Δt = Time difference between successive points on the c-t curve - min
- σ = General stress value on s-t curve - ksi
- σ_1 = Local stress at the crack tip - ksi
- σ_f = Fracture stress for a selected t on s-t curve - ksi

I. INTRODUCTION

The use of glass fiber-reinforced plastics in a marine environment has grown considerably in recent years. Among other uses in this field, it has applications as varied as a structural hull material, a non-structural fairing to hull shapes, and as a topside deck housing material because of its high strength to weight ratio and easy maintenance. (1, 2). Generally speaking, however, it is still a relatively new material for engineering work in the marine environment and more information on its performance characteristics is needed at this time. One aspect of the behavior of FRP is the feasibility of the application of fracture mechanics to the material and the modifications to this theory that are necessary. With the proper adjustments, fracture mechanics has been used in recent studies to predict fatigue crack propagation rates. (3, 4, 5).

The fatigue crack propagation rate was shown by Mandell and Meier (4) to vary approximately with the eleventh power of stress intensity factor for cross-plyed Scotchply (a pre-preg, unidirectional ply, glass reinforced epoxy). More recently it was shown that a number of different glass-reinforced laminates exhibit fatigue crack propagation rates that vary exponentially with stress intensity over the exponent range of 9 to 13. (5). For metals, it is known that dc/dN varies with K_I exponentially, but usually in the range of 3 - 6. (6). The initiation of static load crack growth in metals has been predicted using a material evaluation technique. These static-case results are expressed as the lowest stress intensity to critical stress intensity ratio below which failure will not occur in a given time. (7). This type of relationship has not been shown to exist for glass composites whose mode of fracture is different.

The method of fatigue crack growth has been identified as the failure of a series of ligaments. The crack grows by propagating rapidly through a discrete ligament and then remains stationary for a number of cycles before advancing again (4).

Glass-reinforced composites are known to exhibit considerable creep under a constant stress. (13). At loads near the UTS of the material, failure occurs in the fibers in a relatively short time; whereas, at a lower load level, failure is not reached for a much longer time. There is a need to study this effect in order to safely and accurately design structures that employ GRP laminates in tension and especially in those instances where notches are an integral part of the design.

The purpose of this study is to initiate an investigation of the effects of constant loading of GRP laminates on crack propagation rates. More specifically, the goals of this work are:

- (1) to determine a strength-time curve for a particular laminate, similar to a S-N curve;
- (2) to experimentally determine crack growth rates as a function of stress intensity factor;
- (3) to study the effects of immersion in distilled water on (a) crack growth rates, and (b) the s-t relationship;
- (4) to develop a method of predicting constant stress crack growth rates from a s-t curve.

The method of approach to this investigation is to use unnotched dogbone shaped specimens in static tension tests to obtain a s-t curve for both a dry and a submerged environment. A three inch by five inch index card specimen is employed in a double cantilever tension test to get crack propagation rates in both a dry and a submerged environment.

II. MATERIALS

The fabrication method used in this study was selected because of the ease of reproducibility of material properties from one laminate plate to another. The details of the fabrication procedure are found in Appendix C.

Initially, the material chosen for testing was a woven roving glass fabric (Style 779 - Stevens Fiberglass Co.) in order to make a comparison with previous studies of fatigue crack propagation rates. (3). A number of specimens of this material were made and tested before it was discarded as unsuitable for a preliminary constant stress crack growth rate analysis. The primary reason for the shift away from this material was the wide range of scatter in data obtained which indicated an excessive number of specimens would be needed to determine significant results. The alternative woven glass fabric selected was Style 181 which had considerably more yarns per inch and would provide less data scatter while still testing the same glass filaments. Since the fabric was different than that used in the fatigue crack growth rate study, the use of a salt water testing environment for comparison was dropped in favor of a distilled water environment due to its greater influence on GRP laminates.

The composite plates were compression molded in a 10" x 17" rectangular mold at 50°C. The laminate plates for the dogbone specimen had 10 layers of the glass fabric; whereas, the index card specimen plates consisted of 36 layers. Both types of specimen employed a polyester resin with methyl ethyl ketone peroxide as a catalytic agent. Previous data has indicated no appreciable thickness effects

so the use of only 10 layers for the dogbone specimens was acceptable.(9)

This fabrication method yielded an average fiber volume fraction of 43.3% for the notched specimens and an average fiber volume fraction of 45.95% for the unnotched specimens. The volume fractions were obtained by conducting burn tests on two one-inch squares from each plate made. The shape and geometry of each specimen are illustrated in Figure 3.

III. EXPERIMENTAL PROCEDURE

The testing of the machined specimens was done on either an Instron Model 1211 Dynamic Cyclor or an Instron Universal Testing Machine. The index card specimens were held with pin grips; whereas, standard wedge action grips were used for the unnotched dogbone specimens. The load level could be preset on the Dynamic Cyclor, but had to be manually adjusted on the Universal Testing Machine which was designed to apply a constant displacement rather than a constant load. One each of the two specimen designs was tested to obtain a rough estimate of the ultimate tensile strengths. As a result, the Dynamic Cyclor was set up for 2000 pounds full scale load for the index card specimens and for 4000 pounds full scale load for the dogbone specimens. The Dynamic Cyclor demonstrated a second order time response in reaching the preset load, but, because the rise time was significantly short compared to most of the testing times, the response was approximated as a step function. The short duration tests (two minutes and less) were conducted on the Universal Testing Machine. A description of all the apparatus used can be found in Appendix D.

The procedure followed for all tests was the same for both the dry and submerged environments except that the water containment system was installed in the latter case. For the purpose of this paper, the dry environment is taken to be that in an uncontrolled laboratory. It should be noted that the large amount of rust associated with submerged testing with this unit in previous tests was not present during the current investigation. The two reasons for this are (i) all the metal surfaces were sprayed with Krylon Silicone Spray (Borden, Inc.) to repel the

water and prevent rust; and (ii) any small amount of rust that did form was not shaken loose from the surface as was caused by the cycling in the fatigue study.

Prior to each test, the Dynamic Cyclor was zeroed, balanced and calibrated and the appropriate load level preset. For the dogbone specimen, the timer unit was started simultaneously as the load was switched to the "on" position. The load, and, therefore, the stress, were recorded along with the time to fracture. The strength-time data is shown in Table 3 for the dry environment and Table 4 for the submerged environment. Three specimens were tested at each load level.

The index card specimens had a stainless steel rule calibrated to .01 inches attached parallel to the direction of crack propagation. Under low magnification the crack length, c , was recorded periodically along with the time. There was considerable difficulty in finding a system to accurately locate the crack tip that would work satisfactorily in the submerged environment. It was decided to record the crack length as the farthest point of complete delamination as this provided a clear and easily visible position, whether dry or submerged. The actual crack length was then obtained by plotting c versus t and then subtracting an appropriate amount from c (the average amount for all curves was .03 inches). This lowered the whole curve for each specimen so that the initial crack length was the precut notch length of one inch at the time $t = 0$. All the data has been corrected by this method and the results for the dry and the submerged environments are tabulated in Tables 1 and 2. Again, a replication factor of three was used. The crack growth rates were determined from the $c - t$ curves graphically as the slope of the tangent line to the curve at a particular value of c .

This method is illustrated in Figure 5, and the results are tabulated in Table 5 and Table 6.

For the short duration tests, the Universal Testing Machine was used and the data was recorded as described above. A part of the test procedure included presoaking three specimens of each type for a period of 40 days prior to testing. The results of these tests are in Tables 2 and 4.

IV. ANALYTICAL METHOD

The method of crack propagation under constant load is one of ligament advance as in the case of fatigue crack propagation. The rate of extension of the main crack can be thought of as the ligament width divided by the number of minutes necessary to fail the ligament. The subcracking that occurs perpendicular to the main crack is not considered a part of the main crack extension. This propagation rate can be obtained experimentally as the slope of the tangent to the crack length versus time curve. One of the purposes of this investigation was to develop a means of predicting the crack growth rate from the information contained in a strength-time curve for the material. This concept is an extension of a theory developed recently by Mandell and Meier for fatigue crack growth. The theory has subsequently been verified for a number of varied composite materials and in a marine environment for fiber reinforced plastics under fatigue loading. (3, 5).

The fundamental basis of the concept being tested here is the hypothesis that the ligament of material at the crack tip fails according to the constant-strength life of an unnotched specimen but at the local stress level at the crack tip. If the strength versus log time to failure curve can be approximated as a straight line over the range of interest, then a linear equation can be written as:

$$\log \left(\frac{t}{t_0} \right) = \frac{\sigma_{f0} - \sigma}{s} \quad (1)$$

where σ_{f0} is the stress to cause failure in some initial time, t_0 , σ is the applied static stress, s is the slope of the s - t curve, and t is the time to failure. We note that the stress in the material at the crack tip must reach the local ultimate stress to cause failure (in some

assumed time) simultaneously as the stress intensity factor reaches the candidate critical stress intensity factor (for that same assumed time of stress history).

In the case of the fatigue crack growth, good agreement was found between theory and experiment when the relationship between stress ratios and stress intensity ratios was assumed linear

$$\sigma_1 = \sigma_{f_0} \left(\frac{K_I}{K_Q} \right). \quad (2)$$

A slight modification to this relationship was used in this investigation by assuming the existence of an exponent, n , where $\frac{1}{3} < n < 3$, which provides an approximately linear equation over the range of interest

$$\sigma_1 = \sigma_{f_0} \left(\frac{K_I}{K_Q} \right)^n. \quad (3)$$

Substituting (3) into (1), the crack growth rate for a ligament width d , and $t_0 = 1$ minute, is

$$\frac{dc}{dt} = \frac{d}{\exp \left(2.3 \frac{\sigma_{f_0}}{s} \left(1 - \left(\frac{K_I}{K_Q} \right)^n \right) \right)}. \quad (4)$$

Any effect of the stress distribution ahead of the crack has been assumed negligible for this initial investigation of the crack growth rate. It should be noted that this same assumption introduced no significant error in the case of fatigue crack growth. (4).

The value of stress intensity factor was determined from the relationship found from boundary collocation (8)

$$K_I = \frac{3.46 P \left(\frac{c}{H} + 0.7 \right)}{BH^{\frac{1}{2}}}. \quad (5)$$

This equation was derived specifically for cleavage specimens with isotropic constants. It introduces a slight error when applied to anisotropic material (a maximum deviation of approximately ten percent), but provides invariant toughness results over varying crack lengths in similar materials. (9, 5). The range of stress intensity factor at any given Δt is shown in Figure 8.

The method for determining from the experimental data the relationship between crack growth rates and stress intensity was to obtain the approximate power relationship from a linear log-log curve. No analytical derivation for the selection of the appropriate n for the dry and submerged tests was used. Instead, a trial and error approach was used to approximate the experimental data.

V. RESULTS

The ligament method of crack growth described in (4) was observed for this material and the ligament width, d , was approximated from the crack length vs. time curves as .02 inches.

The unnotched specimens produced nearly linear s - t curves for both the dry and submerged environments. The linearization of these curves yielded, for an initial time of one minute for each, a value for σ_{f_0} of 40.275 ksi and a slope value, s , of 1.969 ksi per decade of minutes for the dry environment and a σ_{f_0} of 42.34 ksi with a slope, s , of 7.52 ksi per decade of minutes for the submerged environment.

The effect of submerging the dogbone specimens was to increase the slope of the s - t curve by a factor of nearly four (actual = 3.82). For an initial time of one minute there is a higher value of σ_{f_0} for the submerged specimens than the dry specimens. This is due to a crossing of the two curves when plotted together at a stress of 39.5 ksi at 2.4 minutes. No significance was attached to this intersection.

The crack growth rate was determined, as described in section IV, to vary with the twenty-fourth power of the stress intensity for the dry specimens. The submerged specimens yielded a twenty-second power dependence of crack growth rate upon stress intensity. The effect of submerging the specimens was to slow the crack propagation. This can be seen in the table below which compares the average total time for the crack to reach four and one half inches for the dry and submerged environments.

<u>Average Load</u>	<u>Average Total Time to Failure</u>		<u>Multiplication Factor</u>
	Dry (min)	Submerged (min)	
1400	33.75	1375.83	40.74
1500	10.42	321.83	30.89
1600	1.44	29.69	20.62

Within the specimens tested in the submerged environment, there was a degree of variation in the crack growth rate curve. At the higher loads where the water had less time to act upon the specimen the results closely approximated the dry environment specimens. When the load was low enough to allow a longer testing time, the slope of the crack growth rate curve was distinct from the dry results initially, but approached the value associated with the dry specimens when the crack began propagating rapidly.

The theory developed does not provide a good approximation to the experimental results for either the dry or submerged case if n is taken as one. As no accurate analytical method exists, the experimental data was approximated by trial and error to yield values for n for the two cases. The data from the dry specimens was best approximated when $n = 0.5$ and the submerged specimens when $n = 2.0$. The selection of K_Q in this theory was made by selecting that value of K_I which corresponded to the initial time, t_0 , as taken from Figure 8.

VI. DISCUSSION OF RESULTS

The linear s-t curves for both the dry and submerged environments are in agreement with previously observed results for the time scale of minutes and hours. (10). The effect of distilled water on the specimens shows a constantly increasing degradation of strength with time for the dogbone specimens. The opposite effect is observed in the index card specimens, where the rate of crack growth is significantly slower at the lower load levels but approaches the dry results at the higher load levels.

Crack growth rate curves in Figure 9 appear to be stacked according to load, rather than overlapping as expected. This indicates that, although the relationship to stress intensity is nearly uniform, the absolute value of the growth rate is dependent upon the load level.

The theory developed in this investigation is unable to predict crack growth rates accurately from the data in a strength-time curve. The theory can provide good results when an additional exponent is added, but this is a questionable procedure unless some other method can be found to confirm that exponent as a material or environmental property.

The use of linear elastic fracture mechanics, and its variations, in the plastic zone in front of a crack propagating under a constant load in metals has provided some methods of predicting the crack growth rates in these metals. Using the concept of stress relaxation of voids, Williams has provided surprisingly similar results to those of McClintock who considered the visco elastic strain history of the zone ahead of the crack (11). Because of the differences in fracture mechanisms, however, these results don't lend themselves to an analogy to our material. The current studies in fracture mechanics of constant load crack growth rates

in metals would probably not provide, then, reasonable results for our composite (12).

Without the existence of theories of crack growth rates for other materials for analogy, and because the theory of Mandell and Meier for fatigue crack growth is very near, in its analogy, to predicting constant load crack growth rates, the concept of altering that theory slightly does appear reasonable. There are several areas where the validity of this theory should be subject to scrutiny. The cumulative effects ahead of the crack might alter the stress field to the point where equation (2) might not be inclusive of the actual stress at the crack tip. The mode of failure of the ligament at the crack tip should also be investigated in view of the apparently significant effects of stress corrosion in blunting of the crack in the submerged tests.

The effects of presoaking had no significant influence upon the s-t curve of the submerged specimens, but decreased the average time to fail the submerged index card specimens by 48%. The amount of surface area, perpendicular to the plane of the fibers, that is exposed to the distilled water, appears to be a significant factor in strength retention and crack growth resistance.

VII. CONCLUSIONS

1. The composite tested produced a linear relationship between the applied stress and the logarithm of the time to fracture over the range of applied stresses. This is consistent with previous results for glass specimens. The submergence in distilled water of these dog-bone specimens increased the slope of the still linear s-t curve which resulted in a constantly decreasing percentage of the time-to-fracture (of a dry specimen) as the stress level was decreased.

2. The crack growth rate under constant load was found experimentally to vary with the twenty-fourth power of the stress intensity factor for dry specimens and with the twenty-second power for those submerged in distilled water. At high load levels, the crack growth rate of the submerged specimens approached that of the dry specimens.

3. The method of crack growth was verified to be one of ligament advance when under a constant load.

4. The length of time that the specimens are exposed to the distilled water prior to testing introduces no significant error for the dogbone specimens, but greatly influences the index card shaped specimens. The average time to fail the presoaked index card specimens was ten times that of those in the dry environment as compared to twenty times as long for those not presoaked but tested while submerged.

5. There is a linear relationship between the stress intensity at the crack tip and the logarithm of the length of time the crack stays at any given length. The slope of this curve is nearly the same for the dry and submerged environments but for any given stress intensity at the crack tip the submerged specimen will remain at that length for a

period of 40 to 50 times that of the dry specimen.

6. The theory developed for predicting the crack growth rate from information obtained in a s - t curve is invalid unless it is altered to include an additional parameter, n . The value of this parameter was determined experimentally to be 0.5 for the dry specimens, and 2.0 for the submerged specimens.

VIII. RECOMMENDATIONS

Very little work has been done in the investigation of constant load crack growth rates in FRP and so this study was aimed at providing some preliminary results as to the nature of these velocities as well as to examine a method of predicting them. There are a number of important areas that emerged from this work which should be studied further in order to more fully understand the fracture of FRP materials in a marine environment.

The shape of the dogbone specimen should be re-evaluated from the viewpoint of stress concentrations to insure that the fracture will occur in the gage section rather than in the transition zone as it did in this study. Higher stress levels should also be used to extend the s-t curve to where the order of magnitude of the time to failure is one to three times less than in the current tests. Such tests would serve to identify the linear region of the stress time curve more clearly as well as help to understand the fracture at the crack tip of the index card specimen when the stress intensity reaches high levels. Where time permits, lower stress levels should also be tested to see if there exists a practical endurance level for this material.

The method of determining the location of the crack tip needs to be investigated in order to reduce the amount of error that was introduced by the method used in this study. The visual method is by far the cheapest and easiest, but other systems (acoustic, electronic, mechanical) should be considered.

The length of time of presoaking before testing should be varied in a series of experiments as this factor contributes significantly to the

crack growth rate. In this same area there are a number of other parameters which were neglected here but which should be included at some future time, such as the type of bath (varied concentrations of acid, or seawater) and temperature.

The theory used to predict the crack growth rates needs to be modified to include other factors so that it might better approximate the experimental data. Further tests are definitely needed to confirm or refute the existence of the additional parameter, n . This parameter may be a material property that varies with time as well as environment. Additionally, this parameter may not exist, in which case, again, the theory needs to be restructured to include those factors which have a significant effect on the crack growth rate. In particular, the mechanism of stress corrosion cracking should be considered in further work in this area. The time dependence of the material properties is important in these time tests and needs to be more completely understood and documented. A key area for further work is the time function of the candidate critical stress intensity since it plays a crucial role in the theory used in this study.

REFERENCES

1. N. Fried and W. R. Graner, "Durability of Reinforced Plastic Structural Materials in Marine Service", Marine Technology, July, 1966.
2. "The Glass Reinforced Plastic Minehunter", Naval Record, October, 1972.
3. R. P. Demchik, "Marine Environment Effects on Fatigue Crack Propagation in GRP Laminates for Hull Construction", S. M. Thesis, M.I.T. Dept. of Ocean Engr., 1973.
4. J. F. Mandell and U. Meier, "Fatigue Crack Propagation in $0^0/90^0$ E-Glass/Epoxy Composites", M.I.T. Dept. of Civil Engr. Report R74-1, 1973.
5. J. F. Mandell, "Fatigue Crack Propagation Rates in Woven and Non-Woven Fiberglass Laminates", to be published, 1974.
6. A. S. Tetelman and A. J. McEvily, Jr., Fracture of Structural Materials, Wiley, 1967.
7. C. C. Osgood, "A Basic Course in Fracture Mechanics", Machine Design Magazine, Penton Publishing Co., 1971.
8. B. Gross and J. E. Srawley, "Stress Intensity Factors by Boundary Collocation for Single-Edge-Notch Specimens Subject to Splitting Forces", NASA Technical Note D-3295, 1966.
9. J. F. Mandell, F. J. McGarry, R. Kashiwara, and W. O. Bishop, "Engineering Aspects of Fracture Toughness: Fiber Reinforced Laminates", M.I.T. Dept. of Civil Engr. Report R73-54, 1973.
10. H. Kolsky and D. Rader, "Stress Waves and Fracture", Fracture, Vol. I, H. Liebowitz, ed., Academic Press, 1968.
11. M. Williams, F. McClintock, Fracture, Vol. III, H. Liebowitz, ed., Academic Press, 1968.
12. F. McClintock, Personal Communication, M.I.T. Dept. of Mech. Engr., May, 1974.
13. L. J. Broutman and R. H. Krock, eds., Modern Composite Materials, Addison-Wesley, 1967.

APPENDICES

	Page
A. Figures	26
B. Tables	37
C. Specimen Fabrication	56
D. Description of Apparatus	58

APPENDIX A.

FIGURES

Figure 1	E-glass Reinforcement. Style 181.
Figure 2(a-b)	Typical Specimen Identification
Figure 3	Specimen Geometry
Figure 4(a-b)	Typical Specimens
Figure 5	Typical Notch Length vs. Time
Figure 6	Strength-Time Curve (Dry Environment)
Figure 7	Strength-Time Curve (Wet Environment)
Figure 8	K_I vs. ΔT
Figure 9	$\frac{dc}{dt}$ vs. K_I (Dry Environment)
Figure 10	$\frac{dc}{dt}$ vs. K_I (Wet Environment)

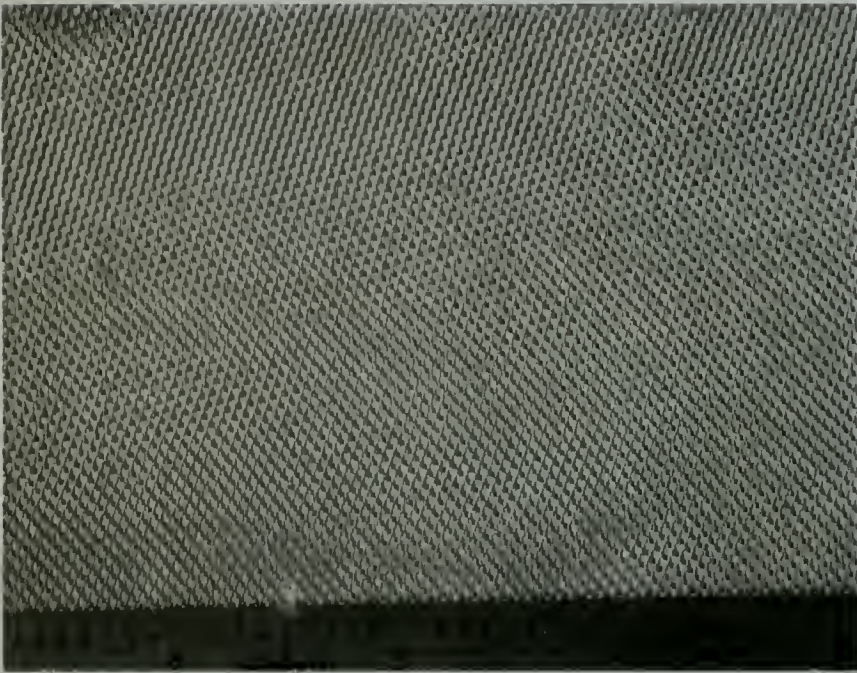
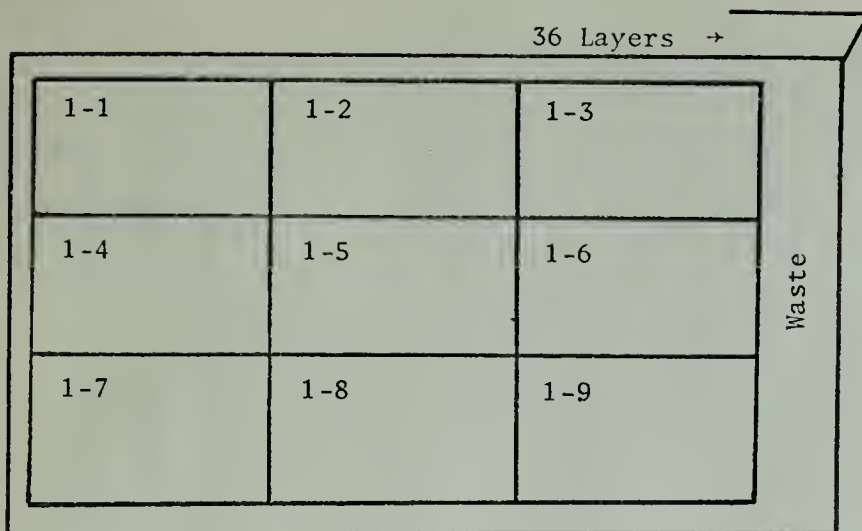
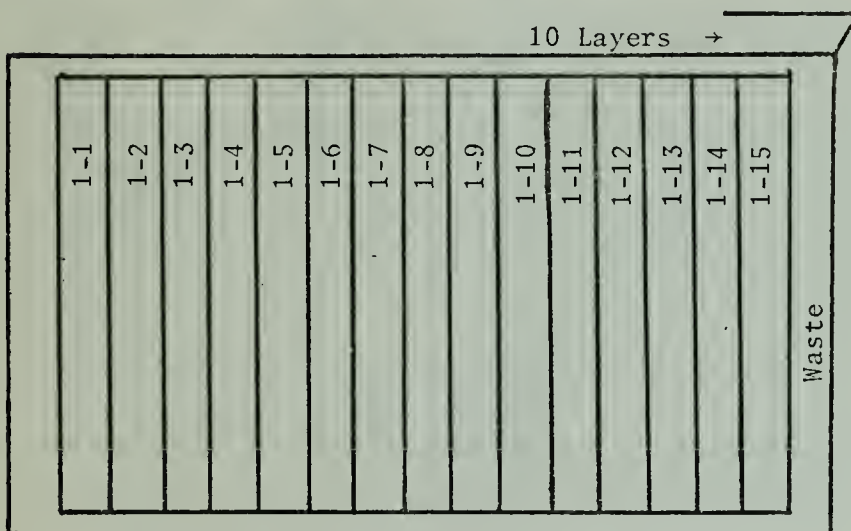


Figure 1. E-glass Reinforcement. Style 181.

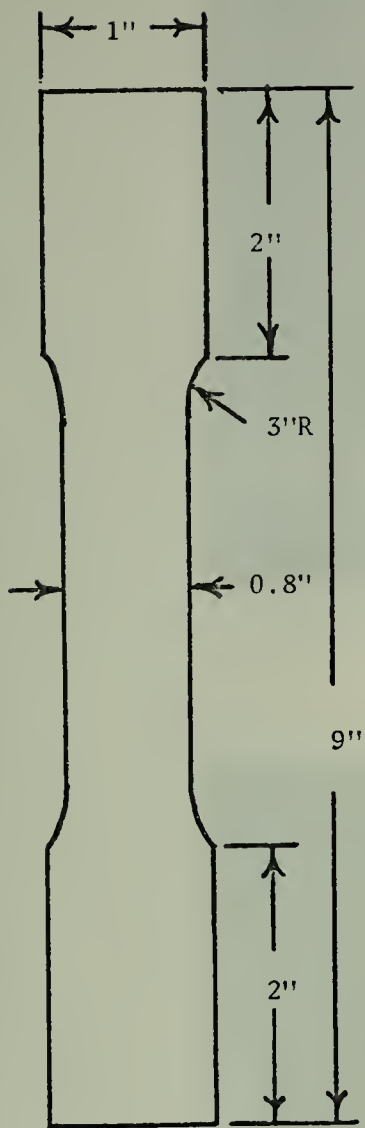


(a) Index Card Numbering

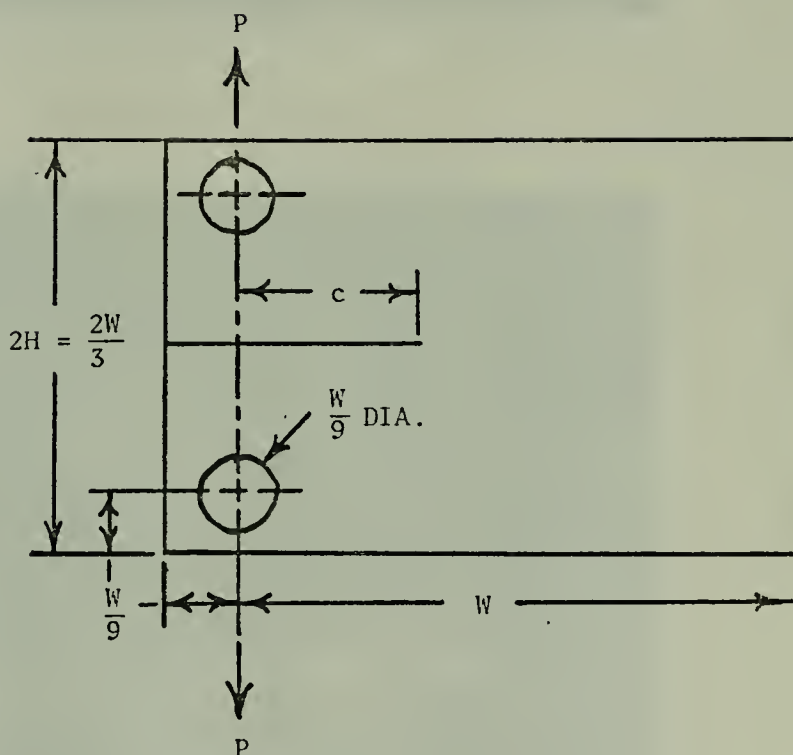


(b) Dogbone Numbering

Figure 2. Typical Specimen Identification

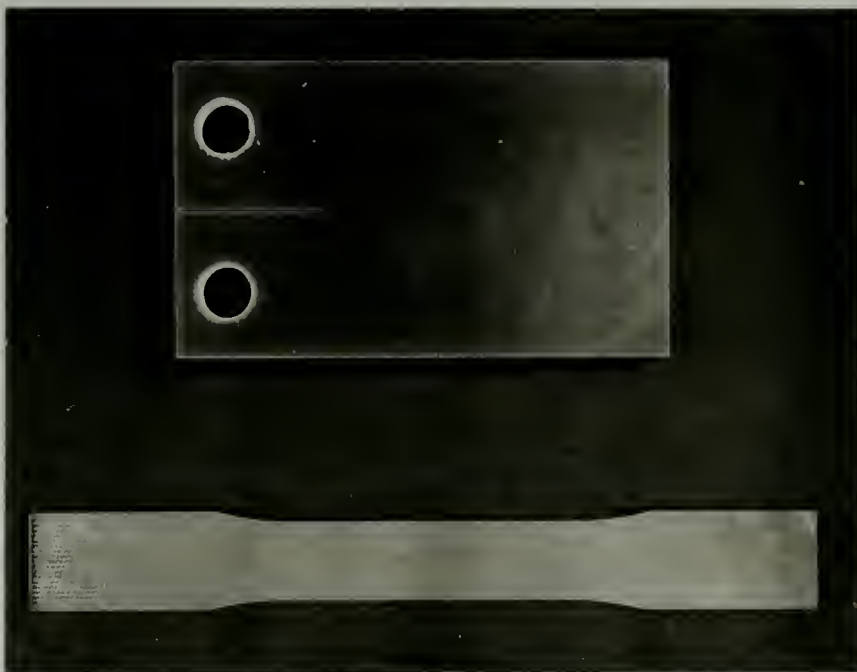


Unnotched
(Dogbone)



Notched
(Index Card)
($W = 4.5$ inches)

Figure 3. Specimen Geometry



(a) Machined Specimens



(b) Specimens After Testing
Figure 4. Typical Specimens

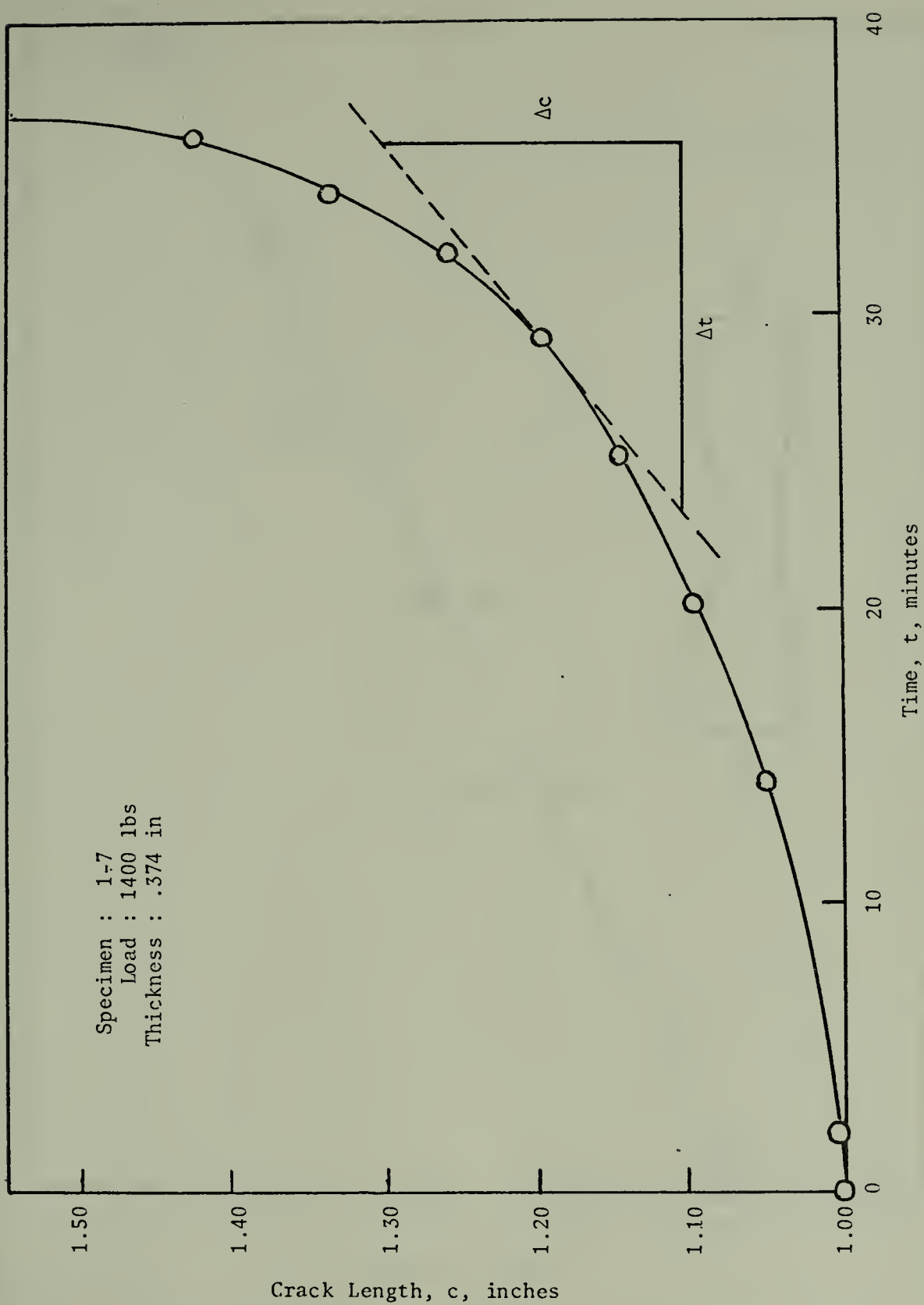


Figure 5. Typical Crack Length vs. Time Curve

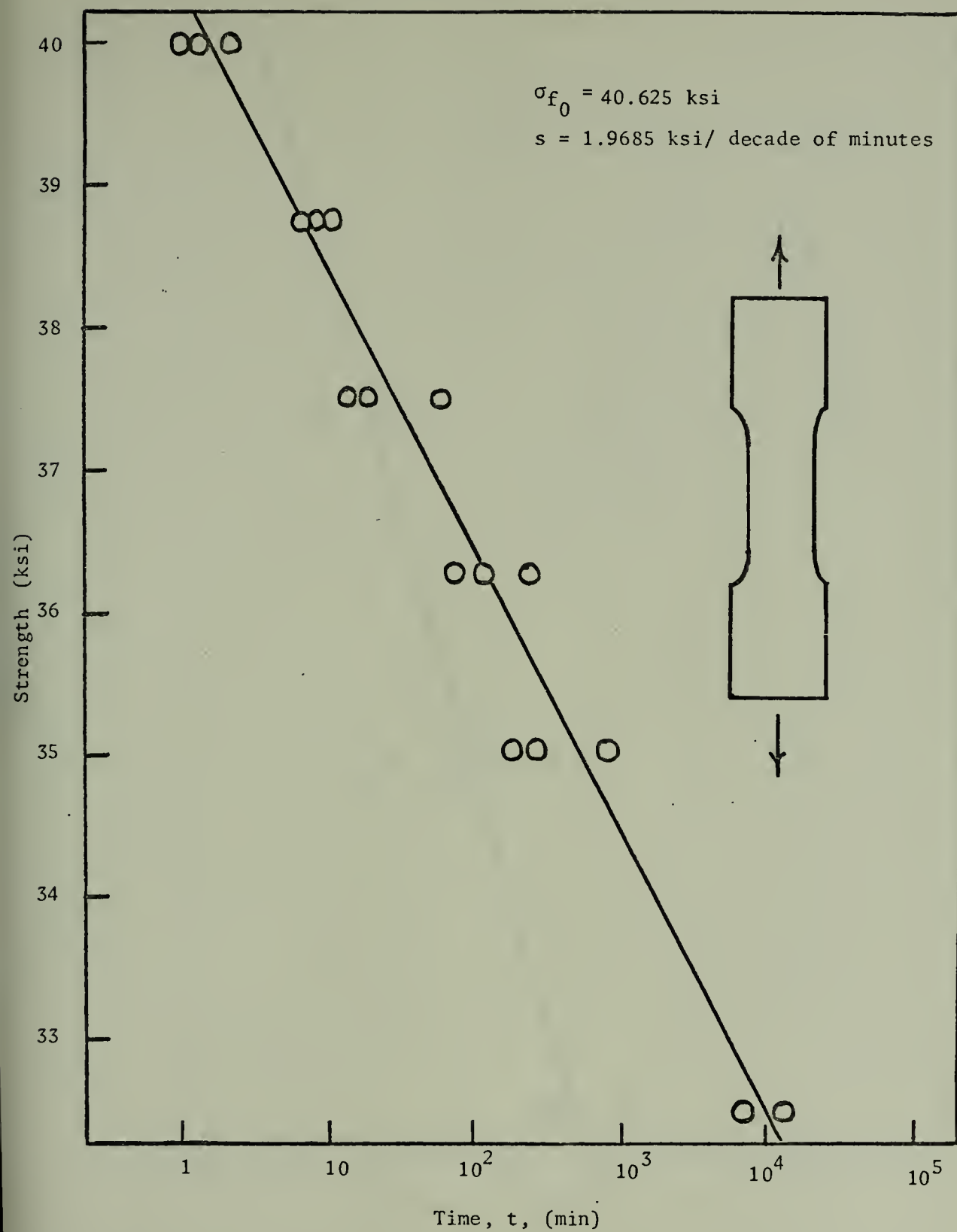


Figure 6. Strength-Time Curve (Dry Environment)

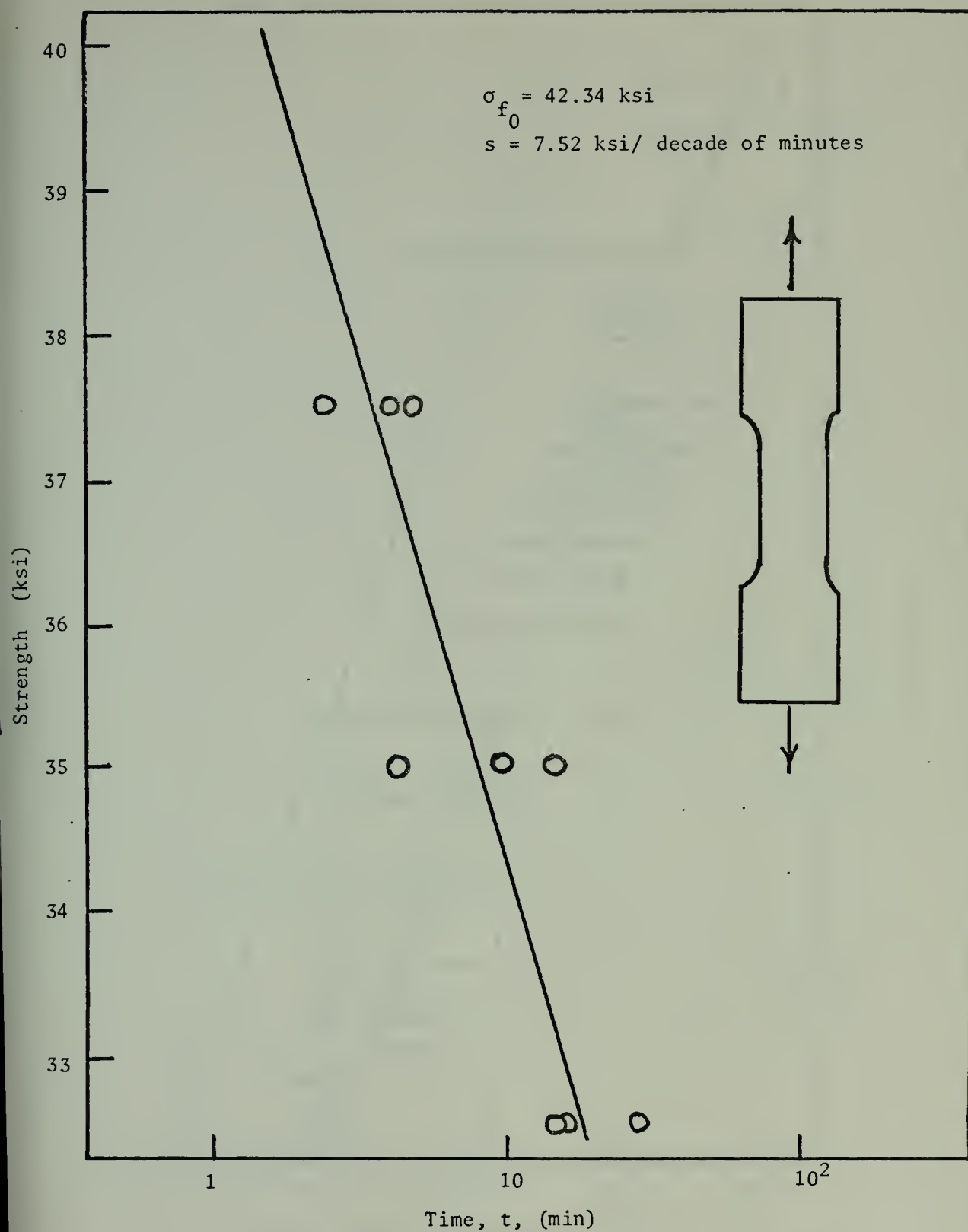


Figure 7. Strength-time Curve (Wet Environment)

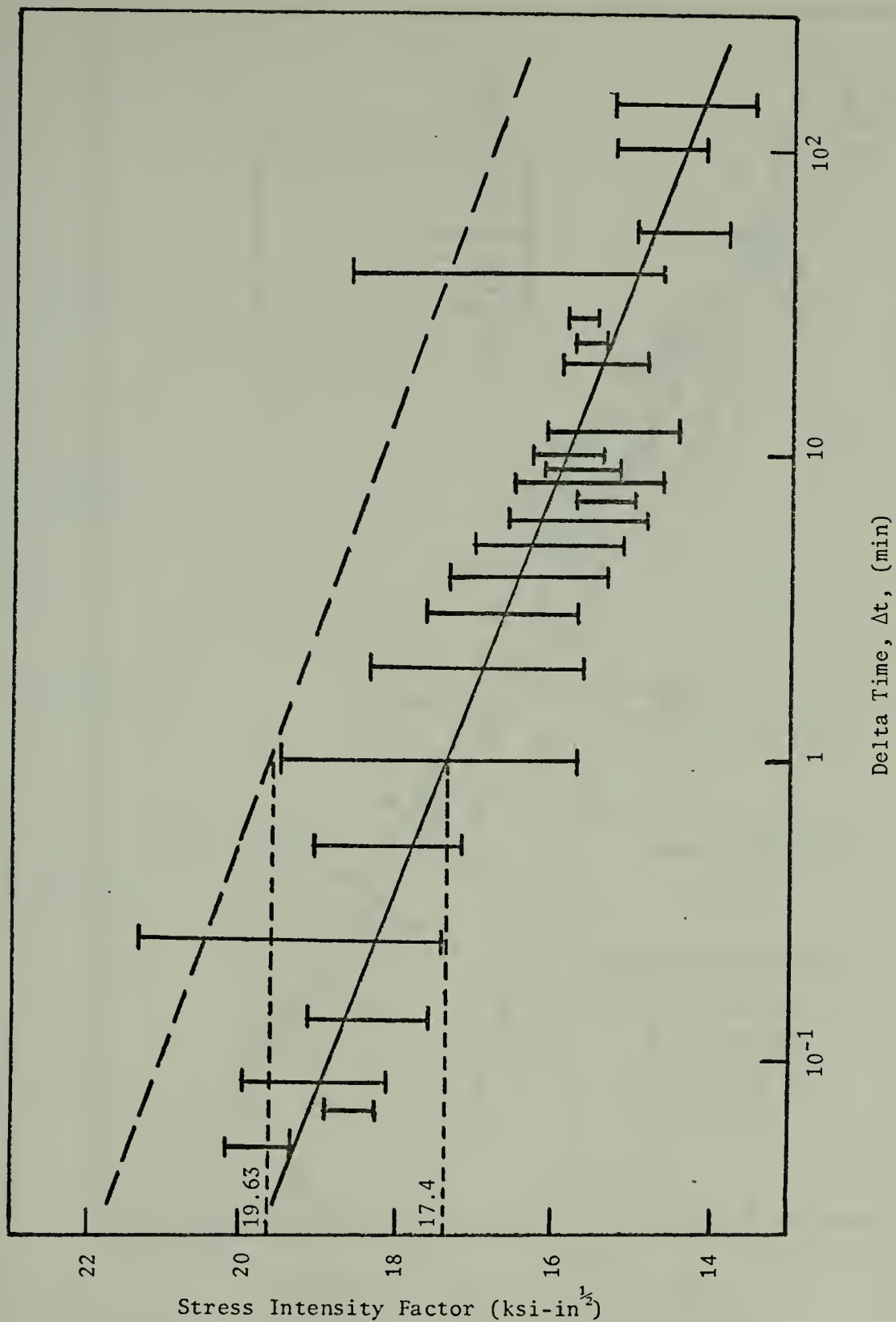


Figure 8. Stress Intensity vs. Delta Time

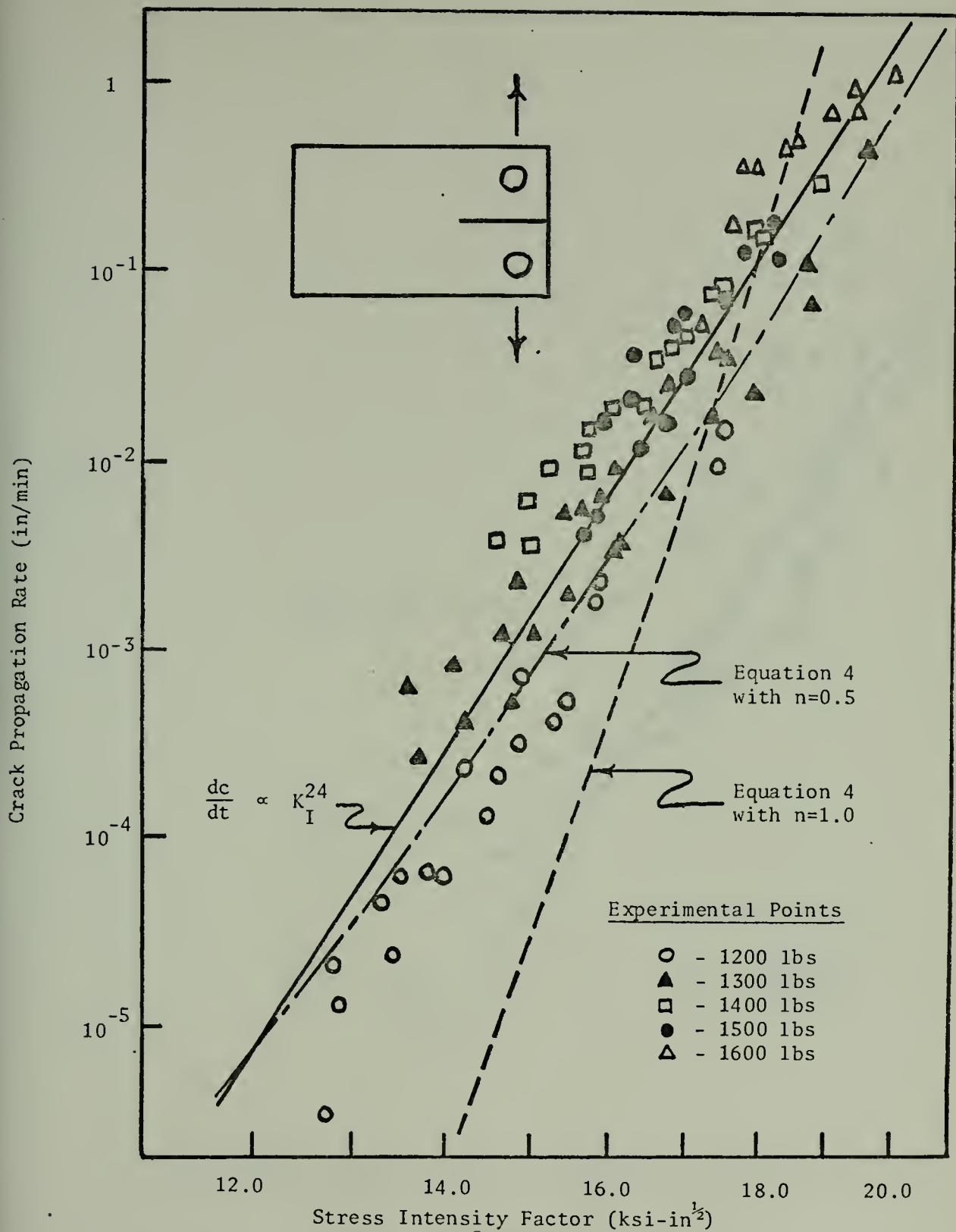


Figure 9. Constant Load Crack Propagation Rate vs. Stress Intensity Factor (Dry Environment)

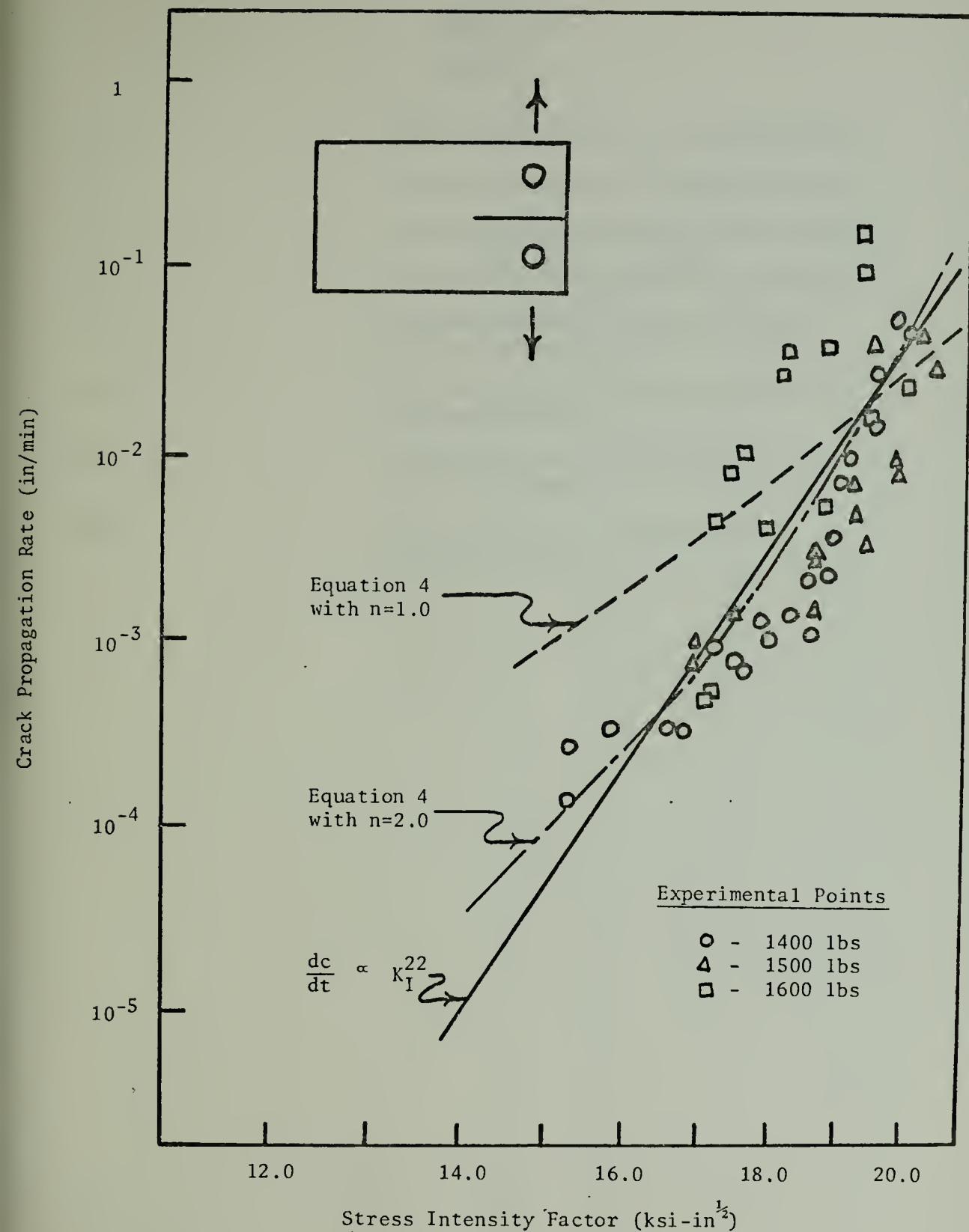


Figure 10. Constant Load Crack Propagation Rate vs. Stress Intensity Factor (Wet Environment)

APPENDIX B.

TABLES

Table 1	Notched Specimen Data (Dry Environment)
Table 2	Notched Specimen Data (Wet Environment)
Table 3	Unnotched Specimen Data (Dry Environment)
Table 4	Unnotched Specimen Data (Wet Environment)
Table 5	Experimental Crack Growth Rate Data (Dry Environment)
Table 6	Experimental Crack Growth Rate Data (Wet Environment)
Table 7	Theoretical Crack Growth Rate Data (Dry Environment)
Table 8	Theoretical Crack Growth Rate Data (Wet Environment)

TABLE 1
NOTCHED SPECIMEN DATA
(DRY ENVIRONMENT)

Load P (lb)	Specimen	Thickness B (in)	Crack Length C (in)	Time t (min)	Delta Time Δt (min)	Stress Intensity Factor K_I (ksi-in ^{1/2})
1200	1-5	.364	1.00	0	1185	12.728
			1.09	1185	795	13.287
			1.15	1980	1020	13.660
			1.21	3000	330	14.032
			1.25	3330	100	14.281
			1.31	3430	50	14.653
			1.35	3480	114	14.902
			1.40	3594	47	15.212
			1.46	3641	28	15.585
			1.51	3669	20	15.895
			1.55	3689	12	16.143
			1.60	3701	13	16.454
			1.65	3714	6	16.764
			1.71	3720	5	17.137
			1.79	3725	3	17.634
			1.86	3728	1	18.068
			1.91	3729	1	18.379
			2.03	3730	1	19.124
			4.50	3731	--	34.460
1200	2-1	.362	1.00	0	630	12.799
			1.001	630	2185	12.805
			1.01	2815	3575	12.861
			1.05	6390	670	13.111
			1.10	7060	640	13.423
			1.13	7700	865	13.610
			1.18	8565	480	13.923
			1.22	9045	655	14.172
			1.31	9700	200	14.734
			1.40	9900	150	15.296
			1.48	10059	40	15.796
			1.56	10090	10	16.295
			1.72	10100	15	17.294
			1.94	10115	40	18.667
			4.50	10155	--	34.650
1200	2-4	.361	1.00	0	5	12.834
			1.001	5	2490	12.840
			1.055	2495	2205	13.179
			1.11	4700	2080	13.523
			1.16	6780	545	13.836

TABLE 1, (Cont'd.)

Load P (lb)	Specimen	Thickness B (in)	Crack Length C (in)	Time t (min)	Delta Time Δt (min)	Stress Intensity Factor K_I (ksi-in ^{1/2})
			1.20	7325	860	14.086
			1.25	8185	370	14.399
			1.30	8555	220	14.712
			1.34	8775	60	14.963
			1.39	8835	115	15.276
			1.44	8950	32	15.589
			1.48	8982	28	15.839
			1.55	9010	18	16.278
			1.64	9028	14	16.841
			1.73	9042	6	17.404
			1.79	9048	3	17.780
			1.88	9051	2	18.344
			1.97	9053	1 $\frac{1}{4}$	18.907
			4.50	9054 $\frac{1}{4}$	---	34.746
1300	1-4	.372	1.00	0	75	13.492
			1.05	75	54	13.821
			1.10	129	91	14.151
			1.16	220	17	14.546
			1.20	237	20	14.809
			1.25	257	21	15.138
			1.30	278	10	15.467
			1.36	288	6	15.862
			1.41	294	4	16.191
			1.46	298	2	16.520
			1.50	300	2	16.783
			1.57	302	3	17.244
			1.68	305	2	17.968
			1.94	307	$\frac{1}{4}$	19.679
			4.50	307 $\frac{1}{4}$	--	36.528
1300	1-9	.371	1.00	0	4	13.529
			1.001	4	144	13.536
			1.05	148	205	13.859
			1.10	353	97	14.189
			1.18	450	36	14.717
			1.25	486	9	15.179
			1.31	495	8	15.575
			1.35	503	7	15.839
			1.40	510	4	16.169
			1.47	514	3	16.631
			1.53	517	3	17.027
			1.62	520	2	17.621
			1.72	522	1	18.281
			2.17	523	$\frac{1}{4}$	21.250
			4.50	523 $\frac{1}{4}$	--	36.627

TABLE 1, (Cont'd.)

Load P (lb)	Specimen	Thickness B (in)	Crack Length C (in)	Time t (min)	Delta Time Δt (min)	Stress Intensity Factor K_I (ksi-in ^{1/2})
1300	2-3	.354	1.00	0	5	14.179
			1.001	5	141	14.186
			1.06	146	107	14.594
			1.12	253	45	15.009
			1.18	298	23	15.424
			1.23	321	23	15.769
			1.29	344	9	16.184
			1.35	353	8	16.599
			1.41	361	3	17.014
			1.47	364	4	17.429
			1.53	368	3	17.844
			1.61	371	2	18.398
			1.77	373	1	19.504
			4.50	374	--	38.386
1400	1-2	.361	1.00	0	1	14.973
			1.001	1	12	14.981
			1.05	13	4	15.338
			1.11	17	3	15.777
			1.16	20	1	16.142
			1.21	21	1	16.507
			1.25	22	1	16.799
			1.28	23	1	17.018
			1.36	24	1	17.603
			1.52	25	1/2	18.771
			4.50	25 1/2	--	40.537
1400	1-7	.374	1.00	0	2	14.453
			1.001	2	12	14.460
			1.05	14	6	14.805
			1.10	20	5	15.158
			1.15	25	4	15.510
			1.20	29	3	15.863
			1.26	32	2	16.286
			1.34	34	2	16.850
			1.43	36	1	17.484
			1.60	37	1/2	18.683
			4.50	37 1/2	--	39.128
1400	1-8	.369	1.00	0	4	14.648
			1.001	4	8	14.657
			1.05	12	7	15.006
			1.10	19	5	15.363
			1.15	24	6	15.720
			1.20	30	4	16.078
			1.26	34	1	16.506

TABLE 1, (Cont'd.)

Load P (1b)	Specimen	Thickness B (in)	Crack Length C (in)	Time t (min)	Delta Time Δt (min)	Stress Intensity Factor K_I (ksi-in ^{1/2})
			1.31	35	1	16.864
			1.36	36	1	17.221
			1.45	37	1	17.864
			1.76	38	$\frac{1}{4}$	20.079
			4.50	38 $\frac{1}{4}$	--	39.658
1500	1-3	.367	1.00	0	2	15.780
			1.001	2	1	15.788
			1.03	3	2	16.011
			1.08	5	1	16.396
			1.10	6	1	16.550
			1.15	7	1	16.935
			1.20	8	1	17.320
			1.34	9	1	18.398
			4.50	10	--	42.723
1500	1-6	.369	1.00	0	1	15.695
			1.001	1	2	15.702
			1.02	3	2	15.848
			1.03	5	1	15.924
			1.04	6	1	16.001
			1.09	7	1	16.384
			1.12	8	1	16.614
			1.19	9	1	17.149
			1.24	10	1	17.532
			1.45	11	$\frac{1}{2}$	19.063
			4.50	11 $\frac{1}{2}$	--	42.491
1500	2-2	.354	1.00	0	1	16.360
			1.001	1	1	16.368
			1.02	2	1	16.519
			1.03	3	1	16.599
			1.05	4	1	16.759
			1.06	5	1	16.839
			1.09	6	1	17.078
			1.12	7	1	17.317
			1.19	8	1	17.876
			1.31	9	.75	18.834
			4.50	9.75	--	44.291
1600	4-4	.362	1.001	0	.883	17.073
			1.05	0.883	.300	17.481
			1.10	1.183	.134	17.897
			1.15	1.317	.066	18.314
			1.20	1.383	.134	18.730

TABLE 1, (Cont'd.)

Load P (lb)	Specimen	Thickness B (in)	Crack Length C (in)	Time t (min)	Delta Time Δt (min)	Stress Intensity Factor K_I (ksi-in ^{1/2})
			1.25	1.517	.133	19.146
			1.35	1.650	.083	19.979
			1.75	1.733	--	23.308
1600	4-6	.358	1.001	0	.583	17.264
			1.05	0.583	.134	17.677
			1.10	0.717	.083	18.097
			1.15	0.800	.133	18.518
			1.20	0.933	.067	18.939
			1.25	1.000	.050	19.360
			1.30	1.050	.033	19.781
			1.35	1.083	.050	20.202
			1.40	1.133	.017	20.623
			1.45	1.150	--	21.044

TABLE 2

NOTCHED SPECIMEN DATA

(WET ENVIRONMENT)

Load P (lb)	Specimen	Thickness B (in)	Crack Length C (in)	Time t (min)	Delta Time Δt (min)	Stress Intensity Factor K_I (ksi-in ^{1/2})
1400	3-3	.363	1.00	0	5	14.891
			1.001	5	350	14.899
			1.06	355	650	15.326
			1.15	1005	280	15.980
			1.21	1285	155	16.416
			1.26	1440	160	16.779
			1.31	1600	97	17.142
			1.37	1697	93	17.578
			1.44	1790	55	18.087
			1.50	1845	25	18.522
			1.55	1870	6	18.886
			1.64	1884	2	19.539
			1.74	1886	1	20.266
			4.50	1887	--	40.314
1400	3-4	.362	1.00	0	8	14.932
			1.001	8	592	14.939
			1.21	600	180	16.461
			1.26	780	52	16.826
			1.32	832	103	17.263
			1.37	935	56	17.627
			1.44	991	37	18.137
			1.49	1028	29	18.501
			1.57	1057	4	19.084
			1.61	1061	3	19.375
			1.69	1064	1	19.958
			4.50	1065	--	40.425
1400	3-5	.358	1.00	0	2	15.099
			1.001	2	119	15.106
			1.03	121	219	15.320
			1.09	340	620	15.762
			1.30	960	68	17.308
			1.35	1028	89	17.676
			1.44	1117	42	18.339
			1.53	1159	6	19.002
			1.58	1165	5	19.370
			1.65	1170	2	19.886
			1.74	1172	$\frac{1}{2}$	20.549
			4.50	1172 $\frac{1}{2}$	--	40.877

TABLE 2, (Cont'd.)

Load P (1b)	Specimen	Thickness B (in)	Crack Length C (in)	Time t (min)	Delta Time Δt (min)	Stress Intensity Factor K_I (ksi-in ^{1/2})
1500	2-6	.358	1.00	0	7	16.177
			1.001	7	33	16.185
			1.05	40	54	16.572
			1.11	94	99	17.045
			1.19	193	100	17.677
			1.26	293	42	18.229
			1.31	335	33	18.623
			1.37	368	4	19.097
			1.41	372	1	19.413
			1.45	373	$\frac{1}{2}$	19.728
			4.50	373 $\frac{1}{2}$	--	43.797
1500	2-7	.363	1.00	0	3	15.954
			1.001	3	167	15.962
			1.18	170	44	17.355
			1.23	214	52	17.744
			1.28	266	55	18.133
			1.33	321	12	18.523
			1.38	333	27	18.912
			1.43	360	17	19.301
			1.49	377	4	19.768
			1.53	381	1	20.079
			1.57	382	1	20.390
1500	2-8	.358	1.00	0	5	16.177
			1.001	5	24	16.185
			1.09	29	36	16.887
			1.14	65	37	17.282
			1.20	102	33	17.755
			1.25	135	30	18.150
			1.32	165	15	18.702
			1.37	180	14	19.097
			1.44	194	11	19.649
			1.53	205	3	20.360
			1.62	208	$\frac{1}{2}$	21.070
1600	2-9	.360	1.00	0	1	17.160
			1.001	1	9	17.168
			1.05	10	9	17.578
			1.09	19	11	17.913
			1.13	30	5	18.248

TABLE 2, (Cont'd.)

Load P (1b)	Specimen	Thickness B (in)	Crack Length C (in)	Time t (min)	Delta Time Δt (min)	Stress Intensity Factor K_I (ksi-in ^{1/2})
			1.15	35	8	18.415
			1.20	43	7	18.834
			1.24	50	5	19.169
			1.32	55	3	19.838
			1.39	58	$\frac{1}{2}$	20.424
			4.50	58 $\frac{1}{2}$	--	46.457
1600	3-1	.361	1.00	0	2	17.112
			1.001	2	9	17.120
			1.08	11	3	17.780
			1.19	14	1	18.698
			1.36	15	$\frac{1}{4}$	20.117
			4.50	15 $\frac{1}{4}$	--	46.328
1600	3-2	.359	1.00	0	2	17.207
			1.001	2	2	17.216
			1.01	4	3	17.291
			1.06	7	2	17.711
			1.07	9	1	17.795
			1.10	10	3	18.047
			1.18	13	1	18.718
			1.22	14	1	19.054
			1.32	15	.33	19.894
			4.50	15.33	--	46.586
1600 (presoaked)	4-7	.360	1.00	0	2	17.160
			1.05	2	5	17.578
			1.09	7	5	17.913
			1.15	12	3	18.415
			1.20	15	1	18.834
			1.31	16	$\frac{1}{2}$	19.755
			4.50	16 $\frac{1}{2}$	--	46.457
1600 (presoaked)	4-8	.361	1.00	0	2	17.112
			1.03	2	3	17.363
			1.07	5	6	17.696
			1.13	11	3	18.197
			1.17	14	1	18.531
			1.22	15	1	18.949
			1.32	16	$\frac{1}{4}$	19.783
			4.50	16 $\frac{1}{4}$	--	46.328
1600 (presoaked)	4-9	.361	1.00	0	2	17.112
			1.04	2	3	17.446
			1.09	5	2	17.863

TABLE 2, (Cont'd.)

Load P (1b)	Specimen	Thickness B (in)	Crack Length C (in)	Time t (min)	Delta Time Δt (min)	Stress Intensity Factor K_I (ksi-in ^{1/2})
			1.10	7	3	17.947
			1.13	10	1	18.197
			1.15	11	1	18.364
			1.20	12	1	18.782
			1.35	13	$\frac{1}{4}$	20.034
			4.50	13 $\frac{1}{4}$	--	46.328

TABLE 3
UNNOTCHED SPECIMEN DATA
(DRY ENVIRONMENT)

Load P (lb)	Specimen	Stress σ (ksi)	Time to Fracture T (min)
3200	2-6	40	1.90
	7-3	40	1.25
	7-4	40	0.90
3100	5-2	38.75	6.6
	5-5	38.75	8.0
	7-1	38.75	10.5
3000	2-3	37.5	16.5
	2-4	37.5	12.75
	2-5	37.5	46.1
2900	7-1	36.25	241
	5-14	36.25	64
	7-5	36.25	128
2800	2-7	35	692
	2-8	35	276
	2-9	35	195
2600	2-10	32.5	5899
	2-11	32.5	10187

TABLE 4UNNOTCHED SPECIMEN DATA

(WET ENVIRONMENT)

Load P (lb)	Specimen	Stress σ (ksi)	Time to Fracture T (min)
3000	7-7	37.5	4.75
	7-11	37.5	5.25
	5-6	37.5	3.05
2800	7-12	35	16.50
	7-13	35	11.25
	7-8	35	5.00
2600	7-9	32.5	14.6
	7-10	32.5	15.4
	5-12	32.5	28.0

(PRESOAKED)

2600	2-13	32.5	37.5
	2-14	32.5	15.0
	2-15	32.5	13.1

TABLE 5
EXPERIMENTAL CRACK GROWTH RATE DATA
(DRY ENVIRONMENT)

Load P	Specimen	Crack Length C	Stress Intensity Factor K _I	Crack Growth Rate $\frac{dc}{dt}$
(1b)		(in)	(ksi-in ^{1/2})	(in/min)
1200	1-5	1.150	13.660	6.61×10^{-5}
		1.257	14.322	2.33×10^{-4}
		1.380	15.088	7.11×10^{-4}
		1.530	16.019	2.33×10^{-3}
		1.793	17.651	1.48×10^{-2}
1200	2-1	1.004	12.822	3.50×10^{-6}
		1.030	12.986	1.37×10^{-5}
		1.093	13.381	4.63×10^{-5}
		1.177	13.902	6.69×10^{-5}
		1.310	14.734	2.11×10^{-4}
		1.440	15.546	5.33×10^{-4}
1200	2-4	1.019	12.951	2.20×10^{-5}
		1.108	13.513	2.44×10^{-5}
		1.203	14.107	6.40×10^{-5}
		1.275	14.555	1.35×10^{-4}
		1.344	14.987	3.21×10^{-4}
		1.415	15.433	4.35×10^{-4}
		1.490	15.902	1.83×10^{-3}
		1.759	17.592	9.77×10^{-3}
1300	1-4	1.025	13.657	6.67×10^{-4}
		1.103	14.173	8.94×10^{-4}
		1.228	14.990	2.41×10^{-3}
		1.330	15.665	6.00×10^{-3}
		1.410	16.191	1.00×10^{-2}
		1.510	16.849	2.75×10^{-2}
		1.625	17.606	3.67×10^{-2}
		1.810	18.824	1.30×10^{-1}
1300	1-9	1.038	13.778	2.83×10^{-4}
		1.177	14.695	1.12×10^{-3}
		1.303	15.531	5.88×10^{-3}
		1.375	16.004	7.14×10^{-3}
		1.467	16.609	1.86×10^{-2}
		1.623	17.643	3.80×10^{-2}
		1.945	19.766	4.50×10^{-1}
1300	2-3	1.020	14.320	4.11×10^{-4}
		1.090	14.802	5.61×10^{-4}

TABLE 5, (Cont'd.)

Load P	Specimen	Crack Length C	Stress Intensity Factor K_I	Crack Growth Rate $\frac{dc}{dt}$
(lb)		(in)	(ksi-in ^{1/2})	(in/min)
		1.150	15.217	1.33×10^{-3}
		1.205	15.597	2.17×10^{-3}
		1.291	16.184	3.75×10^{-3}
		1.380	16.807	7.50×10^{-3}
		1.471	17.429	1.71×10^{-2}
		1.570	18.121	2.67×10^{-2}
		1.690	18.951	8.00×10^{-2}
1400	1-2	1.017	15.097	3.80×10^{-3}
		1.107	15.752	1.61×10^{-2}
		1.225	16.617	3.77×10^{-2}
		1.320	17.311	8.00×10^{-2}
		1.440	18.187	1.60×10^{-1}
1400	1-7	1.026	14.633	4.08×10^{-3}
		1.113	15.255	1.00×10^{-2}
		1.175	15.687	1.25×10^{-2}
		1.230	16.075	2.00×10^{-2}
		1.343	16.873	4.26×10^{-2}
		1.515	18.084	1.70×10^{-1}
1400	1-8	1.050	15.009	6.60×10^{-3}
		1.147	15.720	9.09×10^{-3}
		1.257	16.483	2.19×10^{-2}
		1.335	17.043	5.00×10^{-2}
		1.405	17.543	9.00×10^{-2}
		1.604	18.972	3.10×10^{-1}
1500	1-3	1.010	15.860	5.50×10^{-3}
		1.069	16.310	2.34×10^{-2}
		1.150	16.935	5.12×10^{-2}
		1.270	17.859	1.25×10^{-1}
1500	1-6	1.007	15.748	4.20×10^{-3}
		1.035	15.963	1.72×10^{-2}
		1.083	16.333	3.56×10^{-2}
		1.183	17.098	6.40×10^{-2}
		1.340	18.298	1.85×10^{-1}
1500	2-2	1.017	16.495	1.20×10^{-2}
		1.047	16.732	1.68×10^{-2}
		1.090	17.078	2.86×10^{-2}
		1.155	17.597	7.00×10^{-2}
		1.250	18.355	1.20×10^{-1}

TABLE 5, (Cont'd.)

Load P	Specimen	Crack Length C	Stress Intensity Factor K_I	Crack Growth Rate $\frac{dc}{dt}$
(lb)		(in)	(ksi-in ^{1/2})	(in/min)
1600	4-4	1.025	17.277	5.55×10^{-2}
		1.075	17.689	1.82×10^{-1}
		1.125	18.106	3.73×10^{-1}
		1.200	18.730	5.00×10^{-1}
		1.300	19.563	7.52×10^{-1}
1600	4-6	1.026	17.471	8.40×10^{-2}
		1.075	17.887	3.73×10^{-1}
		1.150	18.518	4.63×10^{-1}
		1.225	19.150	7.46×10^{-1}
		1.276	19.571	1.00×10^0
		1.350	20.202	1.21×10^0

TABLE 6
EXPERIMENTAL CRACK GROWTH RATE DATA
(WET ENVIRONMENT)

Load P	Specimen	Crack Length C	Stress Intensity Factor K_I	Crack Growth Rate $\frac{dc}{dt}$
(lb)		(in)	(ksi-in ^{1/2})	(in/min)
1400	3-3	1.053	15.274	1.49×10^{-4}
		1.260	16.779	3.17×10^{-4}
		1.373	17.602	6.84×10^{-4}
		1.512	18.609	1.09×10^{-3}
		1.563	18.982	3.59×10^{-3}
		1.690	19.903	5.00×10^{-2}
1400	3-4	1.118	15.790	3.43×10^{-4}
		1.317	17.239	9.36×10^{-4}
		1.405	17.882	1.25×10^{-3}
		1.465	18.319	1.35×10^{-3}
		1.530	18.793	2.26×10^{-3}
		1.590	19.230	1.00×10^{-2}
1400	3-5	1.650	19.667	2.67×10^{-2}
		1.030	15.322	2.65×10^{-4}
		1.195	16.535	3.39×10^{-4}
		1.325	17.492	7.35×10^{-4}
		1.395	18.008	1.01×10^{-3}
		1.485	18.671	2.14×10^{-3}
1500	2-6	1.555	19.186	7.14×10^{-3}
		1.615	19.628	1.40×10^{-2}
		1.695	20.218	4.50×10^{-2}
		1.102	16.981	9.05×10^{-4}
		1.313	18.650	3.07×10^{-3}
		1.390	19.255	7.50×10^{-3}
1500	2-7	1.430	19.571	4.00×10^{-2}
		1.138	17.030	1.05×10^{-3}
		1.355	18.718	1.60×10^{-3}
		1.460	19.535	3.53×10^{-3}
		1.510	19.924	1.00×10^{-2}
		1.573	20.416	4.50×10^{-2}
1500	2-8	1.170	17.519	1.51×10^{-3}
		1.313	18.650	2.67×10^{-3}
		1.405	19.373	5.00×10^{-3}
		1.485	20.005	8.18×10^{-3}
		1.575	20.715	3.00×10^{-2}

TABLE 6, (Cont'd.)

Load P	Specimen	Crack Length C	Stress Intensity Factor K_I	Crack Growth Rate $\frac{dc}{dt}$
(lb)		(in)	(ksi-in ^{1/2})	(in/min)
1600	2-9	1.105	18.039	4.12×10^{-3}
		1.197	18.806	5.72×10^{-3}
		1.280	19.504	1.55×10^{-2}
		1.355	20.131	2.40×10^{-2}
1600	3-1	1.0005	17.116	5.00×10^{-4}
		1.040	17.450	8.78×10^{-3}
		1.139	18.274	3.67×10^{-2}
		1.275	19.408	1.70×10^{-1}
1600	3-2	1.0005	17.212	5.00×10^{-4}
		1.006	17.254	4.50×10^{-3}
		1.047	17.599	1.20×10^{-2}
		1.117	18.187	2.75×10^{-2}
		1.200	18.886	4.00×10^{-2}
		1.270	19.474	1.00×10^{-1}

TABLE 7
THEORETICAL CRACK GROWTH RATE DATA
(DRY ENVIRONMENT)

($\sigma_f = 40.625$ ksi; $s = 1.9685$ ksi per decade of minutes; $K_Q = 17.4$ ksi-in $^{1/2}$; $n = 0.5$)

K	$\exp \left[2.3 \frac{\sigma_f}{s} \left(1 - \left\{ \frac{K}{K_Q} \right\}^n \right) \right]$	$\frac{dc}{dt}$
(ksi-in $^{1/2}$)	(minutes)	(in/min)
12	3126.85	6.40×10^{-6}
13	625.26	3.20×10^{-5}
14	132.87	1.51×10^{-4}
15	29.82	6.71×10^{-4}
16	7.026	2.85×10^{-3}
17	1.7312	1.16×10^{-2}
18	0.4442	4.50×10^{-2}
19	0.1183	1.69×10^{-1}
20	0.0326	6.13×10^{-1}
21	0.00928	2.16

TABLE 8

THEORETICAL CRACK GROWTH RATE DATA

(WET ENVIRONMENT)

($\sigma_f = 42.34$ ksi; $s = 7.52$ ksi per decade of minutes; $K_Q = 19.63$ ksi-in $^{1/2}$;
 $n = 2.0$)

K (ksi-in $^{1/2}$)	$\exp \left[2.3 \frac{\sigma_f}{s} (1 - \{ \frac{K}{K_Q} \}^n) \right]$ (minutes)	$\frac{dc}{dt}$ (in/min)
15	218.84	9.14×10^{-5}
16	77.211	2.59×10^{-4}
17	25.4707	7.85×10^{-4}
18	7.8563	2.55×10^{-3}
19	2.2657	8.83×10^{-3}
20	0.6109	3.27×10^{-2}
21	0.1540	1.30×10^{-1}

APPENDIX C

SPECIMEN FABRICATION

Compression molding was used to fabricate the GRP plates in order to provide uniformity among the specimens. The E-glass reinforcement (Style 181; 57 yarns per inch warp, 54 yarns per inch fill; 8.94 oz/yd²; satin weave--Uniglass, Ind.) was supplied with a polyester compatible finish by the manufacturer (Fig. 1). The fabric was cut from 38 inch wide roll into sections measuring 9.75 inches by 16.5 inches to fit into the mold. Two sheets of mylar of the appropriate size were used as outer covering to protect the press and the male half of the mold, as well as to yield a smooth specimen which could easily be removed. The female half of the mold was sprayed with Frekote Mold Release Agent to facilitate easy removal.

The resin (number 4155 Laminac Polyester resin--American Cyanamid Company) was weighed in a one-gallon container. Methyl ethyl ketone peroxide (Specialty Chemicals Division; Reichald Chemicals, Inc.) was weighed in a separate container in an amount equal to 0.5% by weight of the resin and then thoroughly mixed with the resin.

The female mold was placed on a mylar sheet on the lower plate of the press and the resin with catalyst was then spread generously inside the mold. Five layers of the fabric were placed on the resin and more resin poured over them. An aluminum roller was used to work the resin into the entire area of the fabric. More resin was added and the process repeated until the desired number of layers was reached (10 layers for the unnotched specimens, 36 layers for the notched specimens). Adequate penetration and uniform distribution of the resin as well as complete wetting of the glass fibers was achieved by firm pressure on the roller.

Another sheet of mylar was placed on top of the uncured plate followed by a layer of aluminum foil for extra protection to the press. For the notched specimens, the male mold was not used and the upper press plate came in contact with the female mold yielding a plate thickness equal to that of the female mold, .363 inches. The appropriate shims were used with the male mold to insure a thickness of 0.10 inches for the unnotched specimens.

The plates of the press were then brought together and the press pressure raised to 50 psi for 5 minutes, then 80 psi for 3 minutes, and finally raised to 250 psi for the purpose of allowing the air and excess resin to be forced slowly out of this highly viscous mixture. Up to this time, the plates of the press were kept cool to retard curing during the lay-up process. The plate temperature was now set at 50°C to promote uniform setting of the resin. The plate was removed from the press after two hours, and then postcured at room pressure and 100°C for two hours. This process yielded notched specimens with an average fiber volume fraction of $43.3\% \pm 1.34\%$ and notched specimens with an average volume fraction of $45.95\% \pm 1.05\%$.

The completed plates were then marked and labeled as shown by example in Figures 2 a and b. The test specimens were machined to the sizes indicated in Figure 3 using a diamond-edged wheel and a Tensil-Kut router. The initial crack was cut with a .025" thick diamond-edged wheel.

In all cases, the weak direction (fill) of the fabric was parallel to the line of action of the applied force so that the crack was propagated parallel to the warp direction. This was to reduce instances of deviation of the crack from the intended direction of propagation. Figure 4 shows some typical specimens after (a) fabrication and (b) testing.

APPENDIX D
DESCRIPTION OF APPARATUS

The apparatus used consisted of an Instron Model 1211 Dynamic Cyclor and an Instron Universal Testing Machine. Additional apparatus included a water containment system for submerged testing and a circulating water presoak bath.

The majority of the testing was performed on the Instron Model 1211 Dynamic Cyclor. This is a self-contained servo-electronic-hydraulic testing instrument capable of automatically maintaining a preset load. Although it is normally used for sinusoidal load cycling, in this case it provided a constant load with no cycling. A feedback system connects the hydraulic ram to which the lower grip assembly is attached to the load-measuring cell attached to the upper grip assembly. Although the load is preset it may be adjusted through the use of a "fine tuner", and is read visually as a percentage of full range with full load ranges of 2000, 4000, and 10,000 pounds available. This machine demonstrated a second order response typical of most servo-hydraulic machinery with a rise time of approximately 30 seconds and a maximum overshoot of about 25%. The time until steady state condition $\pm 5\%$ was about 75 seconds and therefore the response was assumed to be a step function for all except the shortest tests. The response times were a function of the precharge pressure of nitrogen gas in the system mechanical capacitor which varied a small amount in the months of testing and so only approximations are given to justify the simplification. The grips used for the unnotched specimens were the common wedge action type, and the grips for the notched specimens, as well as general views of the Dynamic Cyclor, have been previously reported (3).

APPENDIX D

DESCRIPTION OF APPARATUS

The apparatus used consisted of an Instron Model 1211 Dynamic Cycler and an Instron Universal Testing Machine. Additional apparatus included a water containment system for submerged testing and a circulating water presoak bath.

The majority of the testing was performed on the Instron Model 1211 Dynamic Cycler. This is a self-contained servo-electronic-hydraulic testing instrument capable of automatically maintaining a preset load. Although it is normally used for sinusoidal load cycling, in this case it provided a constant load with no cycling. A feedback system connects the hydraulic ram to which the lower grip assembly is attached to the load-measuring cell attached to the upper grip assembly. Although the load is preset it may be adjusted through the use of a "fine tuner", and is read visually as a percentage of full range with full load ranges of 2000, 4000, and 10,000 pounds available. This machine demonstrated a second order response typical of most servo-hydraulic machinery with a rise time of approximately 30 seconds and a maximum overshoot of about 25%. The time until steady state condition $\pm 5\%$ was about 75 seconds and therefore the response was assumed to be a step function for all except the shortest tests. The response times were a function of the precharge pressure of nitrogen gas in the system mechanical capacitor which varied a small amount in the months of testing and so only approximations are given to justify the simplification. The grips used for the unnotched specimens were the common wedge action type, and the grips for the notched specimens, as well as general views of the Dynamic Cycler, have been previously reported (3).

For the short time tests, the Instron Universal Testing Machine was used in its manual mode. This is a constant displacement machine in that the moving cross arm travels at a fixed rate and the load cell senses the load variation with time so that the out-put of the chart recorder is load versus displacement. This machine was used as a constant load machine by manually controlling the speed of the cross arm over the range zero to 20 in/min in order to maintain a constant load out-put on the chart recorder. After several trial runs, this was a relatively easy task.

The circulating water presoak bath was used to soak six specimens for a forty day period prior to testing. It consisted of a three gallon polyurethane pail with enough distilled water to cover the specimens. An electric motor driven pump was used to circulate the water on a continuous basis. Distilled water was added periodically to compensate for evaporation losses.

A specially-designed water containment system had already been built for installation on the Dynamic Cyclor and minor modifications were made to it to allow for the use of a different gripping assembly than it was designed to accommodate. The system was a five sided rectilinear box made of 3/8" plexiglas, open at the top and with a hole in the bottom through which the grip holders were threaded into the moveable lower ram of the Dynamic Cyclor. Water-tight integrity was maintained at the hole by using a 1-3/4" rubber O-ring and a 5" diameter nut. The box was assured water-tightness by dismantling it, recoating all the mating surfaces with RTV silicone rubber adhesive/sealant (General Electric Co.), and reassembling it.

A special timing device was constructed to record the time at

which an unnotched specimen failed. It consisted of an electric clock with day, hour, minute, and second indicators and a switching device. When the specimen broke, and the ram lowered the lower grips, this switch created an open circuit and thus stopped the clock. Lag time between failure and clock stoppage was less than four seconds.

Thesis
B242346 Bartron

153002

Fracture of FRP in
marine applications:
constant load crack
propagation.

26 SEP 74

DISPLAY

Thesis
B242346 Bartron

153002

Fracture of FRP in
marine applications:
constant load crack
propagation.

thesB242346

Fracture of FRP in marine applications :



3 2768 002 01493 8

DUDLEY KNOX LIBRARY